Three-axis magnetic flux leakage in-line inspection simulation based on finite-element analysis*

Feng Jian(冯 健)†, Zhang Jun-Feng(张峻峰), Lu Sen-Xiang(卢森骧), Wang Hong-Yang(王宏阳), and Ma Rui-Ze(马瑞泽)

School of Information Science & Engineering, Northeastern University, Shenyang 110819, *China*

(Received 25 May 2012; revised manuscript received 19 July 2012)

With the increase of pipelines, corrosion leakage accidents happen frequently. Therefore, nondestructive testing technology is important for ensuring the safe operation of the pipelines and energy mining. In this paper, the structure and principle of magnetic flux leakage (MFL) in-line inspection system is introduced first. Besides, a mathematic model of the system according to the ampere circuit rule, flux continuity theorem, and column coordinate transform is built, and the magnetic flux density in every point of space is calculated based on the theory of finite element analysis. Then we analyze and design the disposition of measurement section probes and sensors combining both three-axis MFL in-line inspection and multi-sensor fusion technology. Its advantage is that the three-axis changes of magnetic flux leakage field are measured by the multi-probes at the same time, so we can determine various defects accurately. Finally, the theory of finite element analysis is used to build a finite element simulation model, and the relationship between defects and MFL inspection signals is studied. Simulation and experiment results verify that the method not only enhances the detection ability to different types of defects but also improves the precision and reliability of the inspection system.

Keywords: magnetic flux leakage in-line inspection, multi-sensor data fusion, sensor disposition, finite element analysis

PACS: 81.70.Ex **DOI:** 10.1088/1674-1056/22/1/018103

1. Introduction

Petroleum and natural gas are two of the main forms of energy existing in the ocean, whose long distance transport is mainly realized by long distance pipelines. With an increase of pipelines, corrosion leakage accidents happen frequently, which causes a serious waste of resources and environmental pollution disasters. Therefore, nondestructive testing technology is important to ensure the safe operation of the pipelines and energy mining.[1]

Magnetic flux leakage (MFL) in-line inspection technology is applied to the detection of many transfer physical media, and is especially effective for iron pipes.[2] First it magnetizes the wall of the pipeline. Then a leakage magnetic field forms in the defective place of the pipe due to the distortion of the pipeline magnetic field. Finally it detects the range and the intensity of the leakage magnetic field through the magnetic susceptibility components and processes digital signals to determine the defect information. But because the magnetic flux leakage testing equipment is huge and complicated, a high-level manufacturing process is needed.[3] Now, the MFL equipment is only made in a handful of large internationally famous nondestructive testing equipment manufacturing companies. The MFL in-line inspection system designed considers many characteristics of the pipeline from information collection to the analysis and processing of the testing data. The pipeline inspection robot can detect in the pipeline in a timely way to prevent the accident ahead of time. Meanwhile it is a kind of nondestructive detection technology, which does not need to damage the measurement pipeline to collect the data. Last but not least, it has the advantage of location accuracy, and can obtain concrete damage degree information.[4]

At present, pipeline detection methods mainly include magnetic flux leakage inspection, ultrasound inspection,[5] ray inspection, swirling inspection, electronic endoscopic and video inspection, and pressure distribution. Compared with the other inspection methods, the advantages of magnetic flux leakage inspection are as follows. The speed of magnetic flux leakage inspection is faster than that of the others. Besides, it is not sensitive to the medium transported in the pipeline and has a high sensitivity to internal defects of the pipeline. In signal processing, the magnetic flux leakage inspection adopts a permanent magnet or DC magnetization method, so there is no high frequency signal and the interference is very small, so it is convenient for signal processing.

Because sensor technology, digital signal processing ability, and the capacity of storage medium are limited, the traditional magnetic flux leakage detectors mainly adopt the uniaxial or biaxial method. As they only use axial and radial magnetic flux leakage signals to confirm the edge feature of defects, the detection precision is not high. We adopt three-axis magnetic flux leakage inspection in our system,[6] and use circumferential magnetic flux leakage signals to improve the

*Project supported by the National Natural Science Foundation of China (Grant Nos. 61273164 and 61034005), the National High Technology Research and Development Program of China (Grant No. 2012AA040104), and the Fundamental Research Funds for the Central Universities, China (Grant No. N100104102).

†Corresponding author. E-mail: fjneu@163.com

© 2013 Chinese Physical Society and IOP Publishing Ltd

detection precision of length, width, and depth of defects.

2. Structure and principle

The MFL in-line inspection detector takes the medium transportation in the pipeline as the advanced power. It can detect pipelines nondestructively and immediately. Figure 1 shows its overall structure. The detector is composed of a dynamic section, a measurement section, a record section, and a battery section. We use universal joints to connect these sections.

The measurement section contains a magnetization device and hall probes. Besides, as the excitation source, the permanent magnet in the magnetization device does not need a current source and has a high magnetic energy product. There are hall elements in the hall probes. The front department connected to the hall element and pipe wall uses high magnetic conductive wear materials. All the probes are closed absolutely. The structure is shown in Fig. 2.

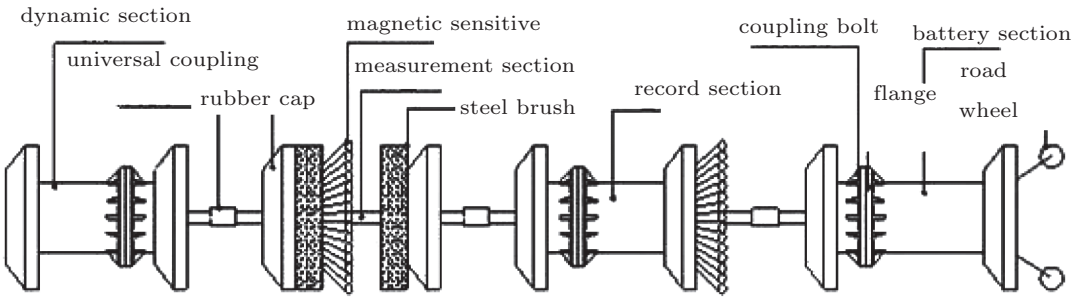


Fig. 1. Overall structure of pipeline magnetic flux internal detector.

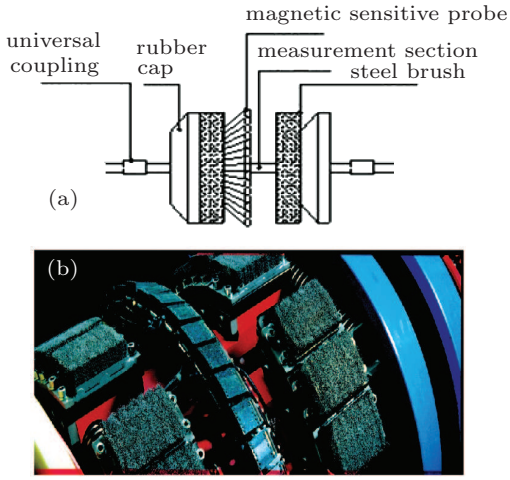


Fig. 2. (color online) (a) Schematic diagram of measurement section, (b) picture of measurement section.

The MFL in-line inspection detector itself carries a permanent magnet. It utilizes the magnet to produce a longitudinal magnetic circuit in the pipe wall circle. When the detector goes forward, if defects do not occur in the pipe wall, magnetic lines of force will be parallel with the wall direction. If defects occur in the outer or inner surface, magnetic lines will traverse through the pipe wall and produce a magnetic flux leakage. As Fig. 3 shows, the leakage magnetic field is between the two magnetic poles, so it will be detected by probes which cling to the pipe wall. Meanwhile, the probes produce corresponding induction signals. These signals will be recorded in memory after being filtered and amplified. Then we judge and analyze the situation by means of data playback and treatment.

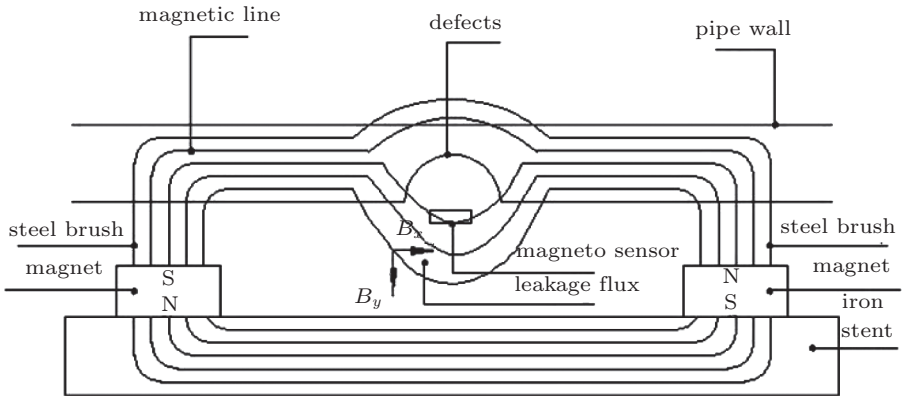


Fig. 3. The principle of MFL inspection.

First we assume that the magnetic properties of the steel pipeline are uniform and isotropic. Namely, material permeability μ of every point in-line is the same, and permeabilities in different directions are identical. According to the structural characteristics (pipeline axisymmetry), we analyze a two-axis static magnetic field. Its Maxwell equation set is[7]

$$\begin{cases} \nabla \times \boldsymbol{H} = J, \\ \nabla \times \boldsymbol{B} = 0, \end{cases} \tag{1}$$

where $\boldsymbol{B}$ is the magnetic flux density vector, $\boldsymbol{J}$ is the equivalent current density, and μ is the material permeability. Due to the magnetic field passivity, we introduce a magnetic potential vector $\boldsymbol{A}$

$$\boldsymbol{B} = \nabla \times \boldsymbol{A}. \tag{2}$$

Because magnetic flux density's divergence identically equals to 0 in Eq. (1), and for any vector function, its curl's divergence identically equals to 0 as well, so

$$\nabla \cdot \boldsymbol{A} = 0. \tag{3}$$

From the above equations, we obtain

$$\nabla \times \left[\frac{1}{\boldsymbol{\mu}} \nabla \times \boldsymbol{A}\right] = \boldsymbol{J}, \tag{4}$$

$$\begin{cases} \boldsymbol{B}_r = -\dfrac{\partial \boldsymbol{A}}{\partial z}, \\ \boldsymbol{B}_z = \dfrac{1}{r} \cdot \dfrac{\partial}{\partial r}(r\boldsymbol{A}). \end{cases} \tag{5}$$

Due to the geometric symmetry, we use the cylindrical coordinate (r, θ, z), then $\boldsymbol{A} = A(r,z)\boldsymbol{e}_0$, where $\boldsymbol{e}_0$ is a unit vector of the $\boldsymbol{H}$ direction. So Eq. (4) can be simplified to

$$\nabla^2 \boldsymbol{A} = \frac{\partial}{\partial r}\left[\frac{1}{r} \cdot \frac{\partial}{\partial r}(r\boldsymbol{A})\right] + \frac{\partial^2 \boldsymbol{A}}{\partial z^2} = -\mu \boldsymbol{J}. \tag{6}$$

Magnetic position vector equation (6) satisfies the Poisson's equation, which belongs to the universal equation. We combine it with boundary conditions to constitute a boundary value problem. It is the mathematical model of function to be solved. For the pipeline, the boundary conditions of the magnetic position vector can be written as follows:

$$\Gamma: \quad \boldsymbol{A} = \boldsymbol{A}_0, \quad \boldsymbol{B}_r = -\frac{\partial \boldsymbol{A}}{\partial r}, \quad \boldsymbol{B}_z = \frac{1}{r} \cdot \frac{\partial}{\partial r}(r\boldsymbol{A}). \tag{7}$$

It is difficult to solve the above mathematical model by using analytical methods. We can set up an energy function which is equivalent to Eq. (6) and seek the minimal value of the function in an approximate function space, and its corresponding boundary conditions are Γ. So we can seek the finite element model solutions of the magnetic flux leakage field in-line, magnetic field intensity, and distribution of magnetic line[8] in every point of space.

3. Acquisition of MFL signals

As the digital signal processing ability is limited, and the memory capacity is finite, most of the previous detectors only record one or two components of three-dimensional leakage magnetic fields. In order to improve these detectors, we can record more components by means of three-axis sensors. Then we can recognize different types of defects and their accurate sizes according to different direction components.

In the magnetic flux leakage signal collection, our system uses the multi-sensor data fusion technique.[9] The basic principle is making full use of multiple sensors by reasonably dominating and combining the multi-sensor data in space and time, then we can get a consistent explanation or description of the detected objects.[10] The goal of data fusion is to enhance the validity of the sensing system by taking advantage of multiple sensors operating collectively. By applying the multi-sensor data fusion technique, our system gets more information of defects on the pipe wall, which can increase the reliability of detection results.

For collecting and reproducing complete defect signals, we put 22 probes around the detector and there are 4 uniformly-spaced sensors in each axial direction of the probe. It can realize detection, tracking, and recognition of magnetic flux leakage, and bring many potential benefits.

One is the improved precision of fusion data. Let n be the number of system sensors in the detection system. The measured mean square errors in the sensors are $\sigma_1, \sigma_2, \ldots, \sigma_n$, respectively. Under the condition that every sensor works independently, it can be proved that after fusion refinement, the measured mean square error of parameters, σ_f, would be

$$\sigma_{\mathrm{f}} = \frac{\sigma^n}{\sigma^{n-1} + \sigma^{n-1} + \cdots + \sigma^{n-1}}. \tag{8}$$

Another benefit is the high reliability and powerful invulnerability. Let the probability of a fault happening to a sensor be p. When there is only one sensor, the reliability of the system is $1 - p$. For a detection system which consists of n independent sensors, we assume that only in the case that all n sensors fail at the same time, the system is paralyzed. According to the probability theory, the probability that n sensors fail at the same time is P^n. So, the reliability of the multi-sensor system is $1 - p^n$.

4. Simulation analysis

4.1. MFL inspection finite-element analysis

The building of the entity model[11] is based on the actual shape of the magnetic flux leakage detection device,[12] as shown in Fig. 4. The distance between the two magnetic poles is 0.17 m; the length of the defect is 10 mm, the depth of the defect is 4 mm on the outer wall; the pipe wall thickness

is 0.009 m, the length is 0.75 m; the magnet is 0.09 m long, 0.025 m thick; and the line iron is 0.35 m long, 0.015 m thick.

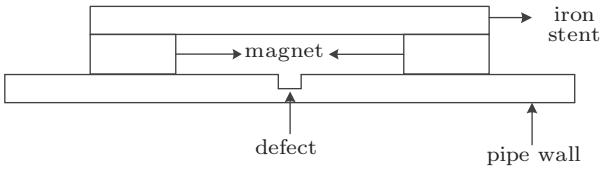


Fig. 4. The entity model.

In the present model, we need to define the materials: air, permanent magnet, line iron, and measured wall.[13] The relative magnetic permeability of the air is 1. The N43 permanent magnetic materials are used, and the magnetic permeability is 1.083. The material of the wall is Q20 low carbon steel, which is widely used in engineering. Its magnetic permeability is 300, its *B*–*H* curve is shown in Fig. 5. For the line iron, we adopt low carbon steel, the magnetic permeability of which is 300.

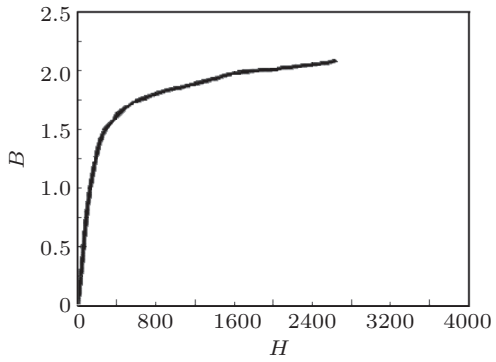


Fig. 5. The *B*-*H* curve of the wall.

We need to define the unit type, material properties, and unit coordinate system for each area before the[1] meshing model.[14] The unit type defined in this model is PLANE97; we set the properties to be axially symmetric. This model belongs to the two-dimensional model and has a relatively small number of degrees of freedom, so we use a linear solver.

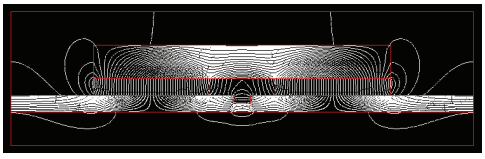


Fig. 6. (color online) Magnetic field distribution at the wall defects.

After it is solved, the two-dimensional magnetic field line figure provided by ANSYS post-processor can show the spatial distribution of the magnetic field wall defects clearly and intuitively, as shown in Fig. 6. The magnetic induction intensity curves along the defect center are shown in Fig. 7(a), the magnetic induction intensity curves along the defect edge are shown in Fig. 7(b). The figures show the radial and axial components of defective magnetic induction in the middle of the two poles.

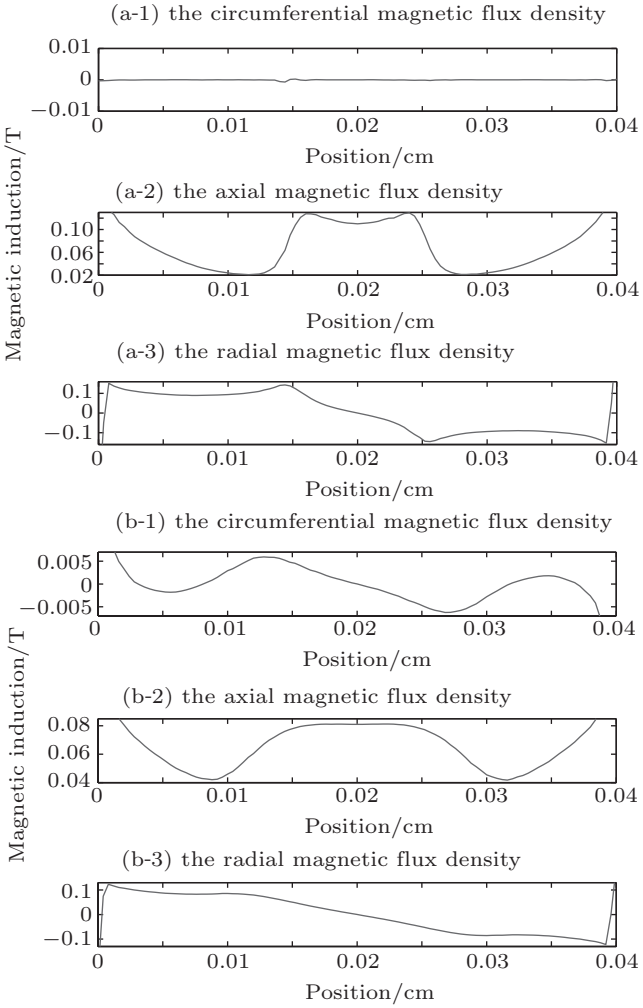


Fig. 7. The magnetic induction intensities along (a) the defect center and (b) the defect edge.

Defects are recognized through the following steps.

(i) Determine the defect form with axial signals. As the axial magnetic flux leakage signals mainly reflect the induction of the wall flux density, their widths have a nonlinear distribution. So according to the axial magnetic flux leakage signals, we roughly estimate the form of the two defects which are nearby and morphologically similar.

(ii) With the radial signals, we further define the length, width, and depth of the defect. The radial magnetic flux leakage signal amplitude has a higher correlation with the depth of the defect; therefore, with the amplitude of the size, we can roughly determine the depth of the defect. The length of the defect can be determined by the radial magnetic flux leakage signal peak position.

(iii) With the circumferential signals we finally determine the defect's size and shape.

4.2. Entity pipeline three-axis testing and analysis

With the previously described finite element analysis of the magnetic flux leakage inspection method,[15] we perform a three-axial magnetic flux density simulation on a surface defect entitative pipeline shown in Fig. 8 and get three axial, radial, and circumferential magnetic induction curves, as shown in Figs. 9–11. Among them, 1#, 2#, and 3# respectively represent the magnetic inductions measured by three sensors, the distance between the sensors is 10 mm.

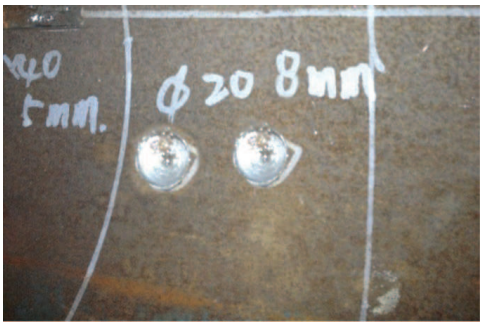


Fig. 8. (color online) The faulty pipeline.

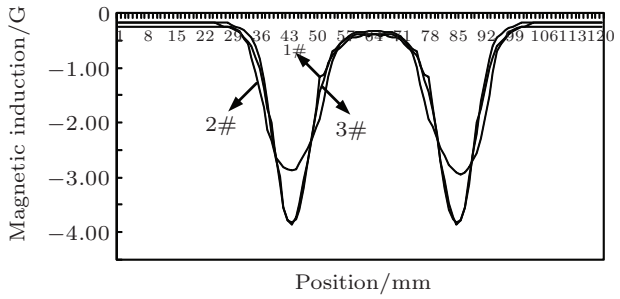


Fig. 9. The axial magnetic flux density curves.

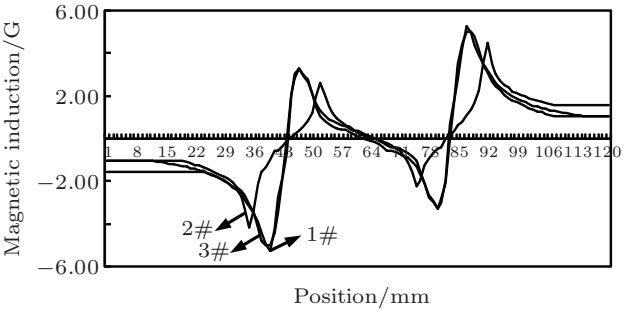


Fig. 10. The radial magnetic flux density curves.

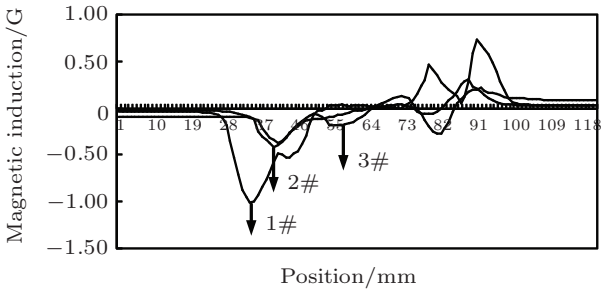


Fig. 11. The circumferential magnetic flux density curves.

With the above magnetic induction curve, we can analyze the defect with the following steps.

(i) With the axial signal amplitude jump,[16] we roughly draw the size of the defect, which is 20.5 mm in length, 19.4 mm in width, and 7.6 mm in depth.

(ii) With the radial signal, we further define the length, width, and depth of the defect. Combining axial signals, we accurately get the maximum depth of the defect (8 mm). Combining the signal amplitude deflections of the radial and the axial magnetic flux leakages, we can draw the basic length of the defect, which is 20.1 mm. By one pair of amplitude basic equal plus or minus two peaks of the radial magnetic flux leakage signal, we can determine the width of the defect to be 19.6 mm.

(iii) With circumferential signals of 1#, 2#, and 3#, we can further determine the length and width of the defect. Combining the axial and the radial components of the measurement results, we obtain the shape of the defect, as shown in Fig. 12. The defect is round, its length and width are 20 mm, and the maximum depth is 8 mm.

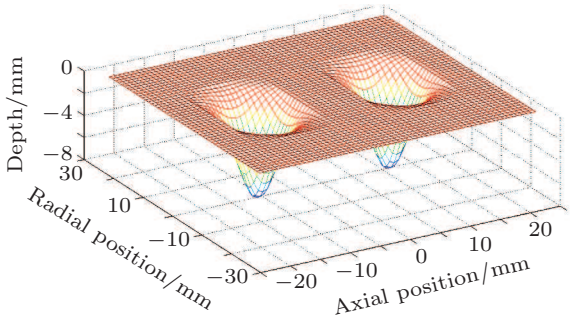


Fig. 12. (color online) Defect identification chart.

5. Conclusion

At present, the MFL signals of the oil and gas pipeline are dealt mainly based on the experience of the testing personnel with excessive human factors, so they cannot meet the requirements of defect evaluation. In this paper, we build a finite element model of a system and show a lot of computer simulation experiments using software ANSYS to deal with the problems existing in MFL quantitative identification. On this basis, we plan to develop a magnetic flux leakage signal pattern recognition technology based on the neural network to improve the objectivity, accuracy, and consistency of signal processing.

References

[1] Silva C E R, Alvarenga A V and Costa-Felix R P B 2010 *Advanced Metrology for Ultrasound in Medicine*, May 12–14, Teddington, UK, **279** 012025

[2] Mandal K, Dufour D, Krause T W and Atherton D L 1997 *J. Phys.* D: *Appl. Phys.* **30** 962

[3] Ryu K S, Atherton D L and Clapham L 2002 *J. Phys.* D: *Appl. Phys.* **35** 2693

[4] Leonard S and Atherton D L 1996 *IEEE Trans. Magn.* **32** 1905

[5] Cès M, Clorennec D, Royer D and Prada C 2010 *Proceedings of the 6th Groupe De Recherche and 9th Anglo–French Physical Acoustics Joint Conference*, January 18–22, Kendal, UK, p. 012017

[6] Mandache C and Clapham L 2003 *J. Phys.* D: *Appl. Phys.* **36** 2427

[7] Bajoni D 2012 *J. Phys.* D: *Appl. Phys.* **45** 313001

[8] Goode P R, Abramenko V and Yurchyshyn V 2012 *Phys. Scr.* **86** 018402

[9] Cheng G W, Zhou Z L, Men Q Y and Deng C N *Proceedings of 2006 International Symposium on Instrumentation Science And Technology*, August 8–12, Harbin, China, p. 1289

[10] Zhang H G, Liu J H, Ma D Z and Wang Z S 2011 *IEEE Trans. Neur. Netw.* **22** 2339

[11] Tasinkevych M, Silvestre N M and Telo da Gama M M 2012 *New J. Phys.* **14** 073030

[12] Wang L M, Luo Y and Ma B K 2002 *Chin. Phys.* **11** 150

[13] Dutta S M, Ghorbel F H and Stanley R K 2009 *IEEE Trans. Mag.* **45** 1966

[14] Hari K C, Nabi M and Kulkarni S V 2007 *IET Sci. Meas. Tech.* **1** 196

[15] Khodayari-Rostamabad A, Reilly J P, Nikolova N K, Hare J R and Pasha S 2009 *IEEE Trans. Magn.* **45** 3073

[16] Gotoh Y and Takahashi N 2002 *IEEE Trans. Magn.* **38** 1209